RevMexAA (Serie de Conferencias), **3**, 199–205 (1995)

THE CYGNUS LOOP: IMPLICATIONS FOR SNR EVOLUTION

John C. Raymond and Salvador Curiel
Harvard-Smithsonian Center for Astrophysics, 60 Garden Street,
Cambridge, MA 02138, USA

RESUMEN

La interacción de una onda explosiva con nubes de mayor densidad en el medio interestelar de baja densidad determina la apariencia y probablemente la evolución de las remanentes de supernova. El "Encaje del Cisne" es un objeto excelente para el estudio de esta interacción. En este artículo discutimos observaciones recientes en rayos X, ultravioleta y óptico de este objeto y sus implicaciones en varios modelos propuestos para explicar dicha interacción.

ABSTRACT

The interaction of a blast wave in low density interstellar gas with higher density clouds determines the appearance and probably the evolution of a supernova remnant. The Cygnus Loop is an excellent target for the study of this interaction. We discuss recent X-ray, UV and optical observations of the Cygnus Loop and their implications for various proposed models of the interaction.

Key words: **ISM: SUPERNOVA REMNANTS — SHOCK WAVES**

1. INTRODUCTION

The simplest model for the evolution of supernova remnants (SNRs) is the Sedov-Taylor self-similar solution for expansion in a uniform medium. There are a few SNRs which are very nearly spherical, such as 0509–67.5 in the LMC, but the vast majority show clear evidence for strong interaction with density inhomogeneities. They depart more or less strongly from spherical symmetry, and they show intensity variations at all wavelengths. The general correlation of X-ray, optical and radio bright spots in all these SNRs naturally results from the interaction of a blast wave in diffuse gas with a dense cloud.

Many different theoretical models have been advanced, each emphasizing a different aspect of the interaction or assuming a different pre-existing density structure. Cox & Smith (1974) considered large scale structures composed of successive SNRs. The higher shock speed in low density gas can channel the energy of supernovae into tunnels of reheated supernova bubbles. The only physical processes in this model are shock heating and radiative cooling. McKee & Ostriker (1977) turned this picture inside out. They considered a pervasive hot, low density medium with dense embedded clouds. In their model, a blast wave in the intercloud gas overruns the dense clouds with little direct effect on the dynamics. However, the clouds evaporate due to thermal conduction, increasing the density and decreasing the temperature of the SNR until radiative cooling sets in. The McKee & Ostriker theory is a consistent picture of SNR evolution and ISM structure. It depends upon the assumption that magnetic fields do not inhibit thermal conduction.

Another set of large-scale models considers the implications of the spatial correlation of supernovae in OB associations. The combined O star winds and supernova explosions can create a superbubble large enough that buoyancy may cause it to break out of the galactic disk, feeding hot gas into the galactic halo (Norman & Ikeuchi 1989) and perhaps driving a galactic fountain (Shapiro & Field 1976). A somewhat analogous "breakout" can occur if the explosion takes place in a dense cloud. Falle & Garlick (1986) have proposed this model for the

Cygnus Loop in order to explain the bright optical filaments on the eastern and western sides, along with the fainter, somewhat larger scale features which encircle the northern part. The classic example of such a breakout is VRO 42.05.01 (Burrows & Guo 1994).

On the next smaller scale are theories pertaining to the interaction of an SN blast wave with a dense cloud comparable in size to the SNR. These include models in which the SN progenitor creates a cavity surrounded by a dense shell, either by photoionization heating for by a powerful wind (Shull et al. 1985; Franco et al. 1991; Arthur & Henney 1995). In these models, the SNR is very underluminous until the blast wave reaches the dense shell. When it does, the transient pressure increase causes a brief period of very high luminosity. The northeast and west portions of the Cygnus Loop are likely to be manifestations of the transient brightening when the blast wave reaches a large, dense cloud. Hester, Raymond, & Blair (1994) and Levenson et al. (1995) have analyzed X-ray, optical and UV observations of these regions to derived density contrasts and other parameters.

Finally, one can focus on the interaction with clouds much smaller than the blast wave radius. As mentioned above, the McKee & Ostriker ISM hinges on thermal evaporation of small clouds. Cox (1981) and Tenorio-Tagle & Różyczka (1986) emphasize "cloud-crushing" —the loss of energy by the radiative shock wave driven into the cloud. More recent models emphasize hydrodynamic stripping of the shocked cloud primarily by Kelvin-Helmholtz instabilities. A model for free expansion in a very low density cavity containing dense clouds (mass-loaded flow) is given by Arthur & Henney (1995). Numerical simulations of a blast wave striking a small spherical cloud are presented by Stone & Norman (1992) and by Klein, McKee, & Colella (1994). These show complete disruption of the cloud on a very short timescale, though a magnetic field might halt the turbulent cascade at small scales (Mac Low et al. 1994; Jones & Kang 1993), and it is not clear how quickly the stripped material will merge with the high temperature gas. Slavin, Shull, & Begelman (1995) present predicted spectra from mixing of cool gas into hot. Fesen, Kwitter, & Downes (1992) pointed out a knot in the southeast Cygnus Loop which seemed to match the numerical models, but X-ray observations and deeper optical imagery show it to be a part of a much larger feature (Graham et al. 1995).

Hester & Cox (1986) analyzed observations of the eastern edge of the Cygnus Loop in an attempt to distinguish among these different pictures. In particular, they examined an apparently triangular feature seen in [O III] and Hα images which they called XA. It is also bright in X-rays, and it is roughly one arcminute long on its east-west axis. Hester & Cox concluded that the X-ray and optical observations were not consistent with the evaporation model which had been proposed for the region by Teske & Kirshner (1985), but that a shocked cloudlet model worked quite well. In this picture, the blast wave drives a slower radiative shock into the cloud, while a reverse shock in the X-ray emitting gas heats and compresses the hot gas just inside the remnant from the dense cloud. This is a transient phase, because the radiative shock quickly traverses the cloud, and because the reverse shock dissipates on a sound crossing timescale. The shocks are related by rough equality of ram pressures, $\rho_o v_s^2$ (McKee & Cowie 1975).

A closely related question is the nature of the filamentary structure observed in the Cygnus Loop and other SNRs. Suggestions over the years have included individual radiative shocks in small clouds (since shown to be incorrect by deeper images which connect the separate filaments, for instance in the northeastern part of the Cygnus Loop), thermal instabilities (Falle 1995) or dynamical instabilities (e.g., Ryu & Vishniac 1987). It is now clear that most of the filamentary structure results from projection effects when one views a very thin, rippled sheet of gas nearly edge-on (Hester 1987), a beautiful example being the non-radiative shocks in the northeast Cygnus Loop (Hester, Raymond, & Danielson 1986). In this case, the ripple could easily arise from very slight ($\leq 10\%$) variations in the ambient density. In radiative shocks, the filamentary structure is less orderly. Seen in [O III], the filaments are generally crisp, while images in Hα and other low ionization lines show fuzzy structure (Fesen, Blair, & Kirshner 1982). While thermal instabilities might produce different morphologies in [O III] and Hα, it is not obvious that they should. Another possibility is that the structure in the recombination zone is governed by the pressure of the magnetic field, and that the field is chaotic. This might be expected, since theories of diffuse shock acceleration of cosmic rays require saturated Alfvén turbulence ($\delta B/B \sim 1$) in the shock precursor. The shock wave compresses the field component parallel to the shock by a factor of four, and this component will be further compressed as the gas cools. Thus the magnetic pressure, and therefore the gas density, should vary strongly within the recombination zone. Dense clumps of gas will be bright in Hα when they are illuminated by ionizing radiation, even if they are somewhat distant from the shock front, so the Hα morphology will be clumpy and irregular.

Several extensions of the Hester & Cox observations have become possible with recent instrumentation. *ROSAT* X-ray images with the HRI and PSPC provide two to three times better spatial and spectral resolution than the Hester & Cox *Einstein* images. Long-slit echelle images reveal the velocity field and ram pressure (see Raymond et al. 1988), and ultraviolet spectra indicate the shock velocity and the degree of depletion in the X-ray emitting gas.

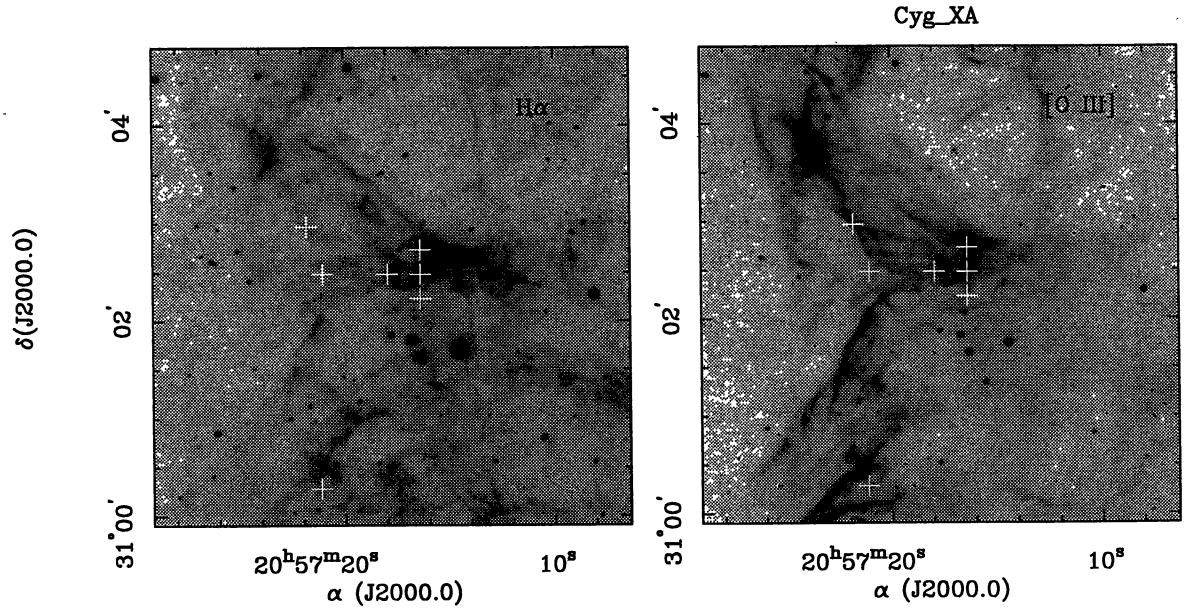

Fig. 1. Hα and [O III] images of XA.

2. OPTICAL DATA

Figure 1 shows Hα and [O III] images of the XA region with positions of it *IUE* observations shown as crosses. The western tip of the triangular feature is several times brighter than the rest of XA, and it is spectrally different as well, showing much lower ratios of high excitation to low excitation lines. In contrast to some other features (Hester, Parker, & Dufour 1984) the spectral difference shows that this is a distinct physical entity, rather than an artifact of projection onto the line of sight. While the [O III] filaments trailing eastward from the head of XA are generally smooth, an Hα image shows considerable disorder.

Long slit echelle spectra have been obtained with the E-W and N-S slits. The E-W spectrum shows that the Hα and N II lines are somewhat clumpy and they both show roughly constant 40 km s^{-1} splitting from the tip to the eastern edge of the feature. The N-S slits show that [O III] is more smoothly distributed than [N II] or Hα, and all the lines show a flattened "velocity ellipse" as expected from the picture of the triangular feature as a conical converging shock. The ellipse is flattened, because the axis is tilted toward the earth. Again, the splitting is about 40 km s^{-1}.

3. X-RAY DATA

Figure 2 shows the X-ray contours from the *ROSAT* HRI image superposed on the [O III] image. Aside from the very small, very bright knot at $20^h57^m20^s, +31°0'10''$, the most obvious feature is the bright X-ray emission surrounding XA, particularly to the north and west. (Note that the contour at $20^h57^m20^s, +31°2'30''$ is a local minimum). A fit to the PSPC spectrum in the square arcminute including XA shows a very low temperature, only 10^6 K. The temperature rises to 2×10^6 K several arcminutes to the west, and it rises toward the north and south as well. A grey scale plot with light grey representing 0.1 keV and the darkest shades 0.3 keV is shown in Figure 3. This confirms the analysis of Hester & Cox, but is even more extreme. The emission measure is about 70 cm^{-6} pc. If silicon and iron are depleted onto grains, the temperature could be still lower and the emission measure higher (Vancura et al. 1993). Comparison of the *ROSAT* fluxes with the [Fe X] flux of Ballet et al. (1989) implies that the product of the fraction of Fe which is Fe X and the depletion of iron compared to the cosmic abundance is about 0.023. Iron is probably moderately depleted in the XA X-ray emitting gas.

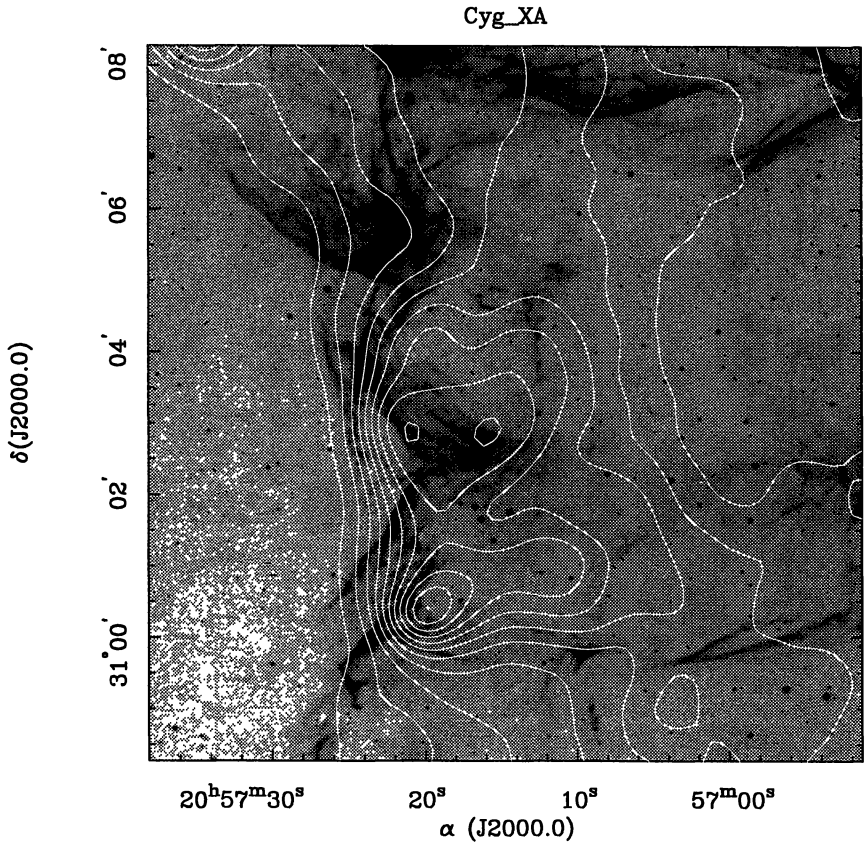

Fig. 2. X-ray contours overlaid on [O III] image.

4. ULTRAVIOLET DATA

Figure 4 shows several ultraviolet spectra obtained with *IUE*. Comparison with models is complicated by resonant scattering of the permitted lines, especially C IV (Cornett et al. 1992), but by combining the *IUE* spectra with [O III] and Hα fluxes measured from the narrow band images, we estimate shock velocities 120 $\leq v_s \leq$ 170 km s^{-1}, with the smallest value near the tip of XA. A shock which has only recently encountered dense gas may not have established a full cooling and recombination zone, and is called incomplete. Detailed analysis based on truncated steady-flow models is risky, but Hα is about half as strong as expected relative to the other lines, indicating that the radiative shock has swept up a column density 18.0 $\leq$ log N_H $\leq$ 19.0, increasing from the eastern end of XA to the tip.

5. INTERPRETATION

We first consider the thermal evaporation picture as an explanation for XA. Teske & Kirshner (1985) favored an evaporative model for the [Fe X] emission from this region, but Hester & Cox (1986) pointed out several difficulties with an evaporative model for the X-ray emission, including the high pressure needed to match X-ray observations and the low observed temperature. The *ROSAT* observations exacerbate the second difficulty, because the X-ray temperature is better determined. They add the difficulty that the temperature gradient is very shallow, and the temperature decreases outwards; opposite to the naive expectation of the

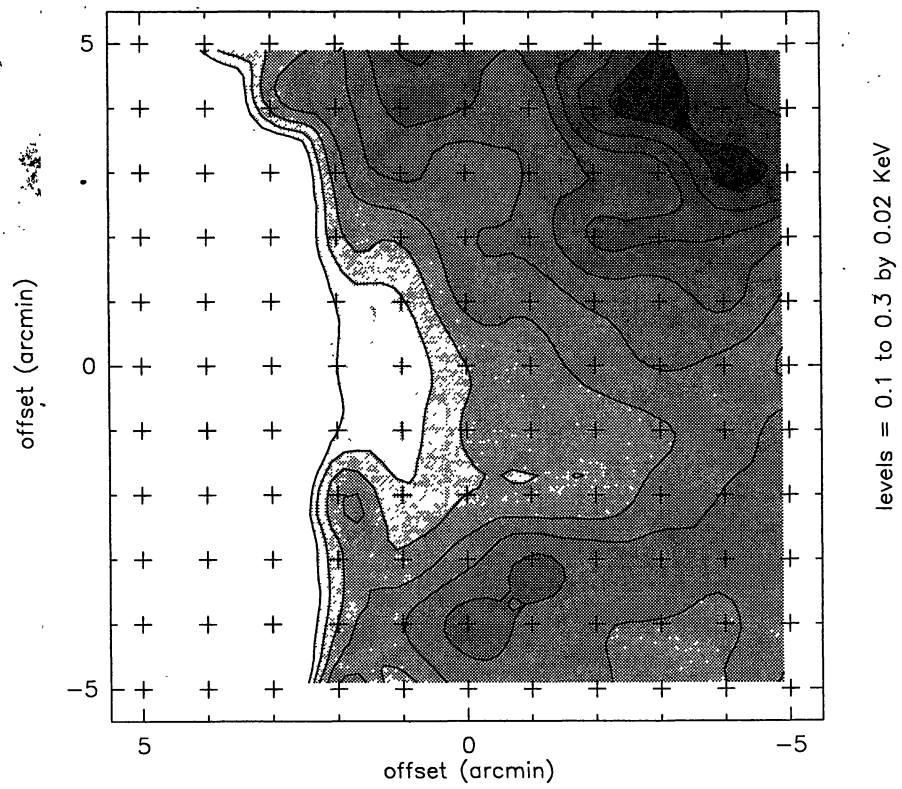

Fig. 3. X-ray temperature map.

evaporative model. The long slit echelle observations suggest that XA is very elongated, significantly reducing the required pressure compared with that derived by Hester & Cox, but the problem remains.

We next consider the turbulent stripping picture. Here, one would expect that more of the cool gas would be mixed in the X-ray-emitting gas farther downstream from the cloud at the tip of XA. Thus the decreasing temperature at the edge is a natural consequence of this picture. The thickness of the X-ray emitting region and the fact that the X-ray enhancement begins upstream from the cloud both present problems, however. The density enhancement due to mixing cool gas into the X-ray producing gas should only occur downstream from the cloud. The thickness of the region suggests a shallow velocity gradient (slow mixing) and at the same time requires efficient mixing over a relatively great distance. J. Hester points out that some wave-like features suggestive of Kelvin-Helmholtz driven turbulence are visible in WFPC-I images of XA, and that our age estimates for the interaction at XA are uncertain, so that there may have been sufficient time to mix cool material throughout the X-ray emitting zone we observe. Therefore, the strongest argument against the mixing picture may be that the timescales estimated from the degree of recombination (determined from [O III]/Hβ ratios) decrease as one goes downstream from the tip of XA, in opposition to the sense expected for a turbulent stripping model but in harmony with a simple shock wave picture.

Finally, we consider a cloud-crushing interpretation, in which the filaments trailing to the east from the tip of XA are simply radiative shocks being driven into material behind the cloud at the tip of XA in the form of a converging cone. The pressure exerted by the X-ray emitting gas is quite large, but the ram pressure of this material is directed eastward, so the ram pressure of the radiative shocks should be smaller than the ram pressure at the tip. Most of the observations fit into this interpretation; the morphology of XA, the X-ray gas pressure, the long slit echelle results, and the decline of n_e toward the east. The complex, bright tip of XA resembles numerical simulations. There are significant difficulties with this picture. The relatively small velocity splitting observed in the echelle spectra implies that the opening angle of the converging conical shock is extremely large, perhaps 160°. This could be avoided if the gas velocity is not perpendicular to the shock

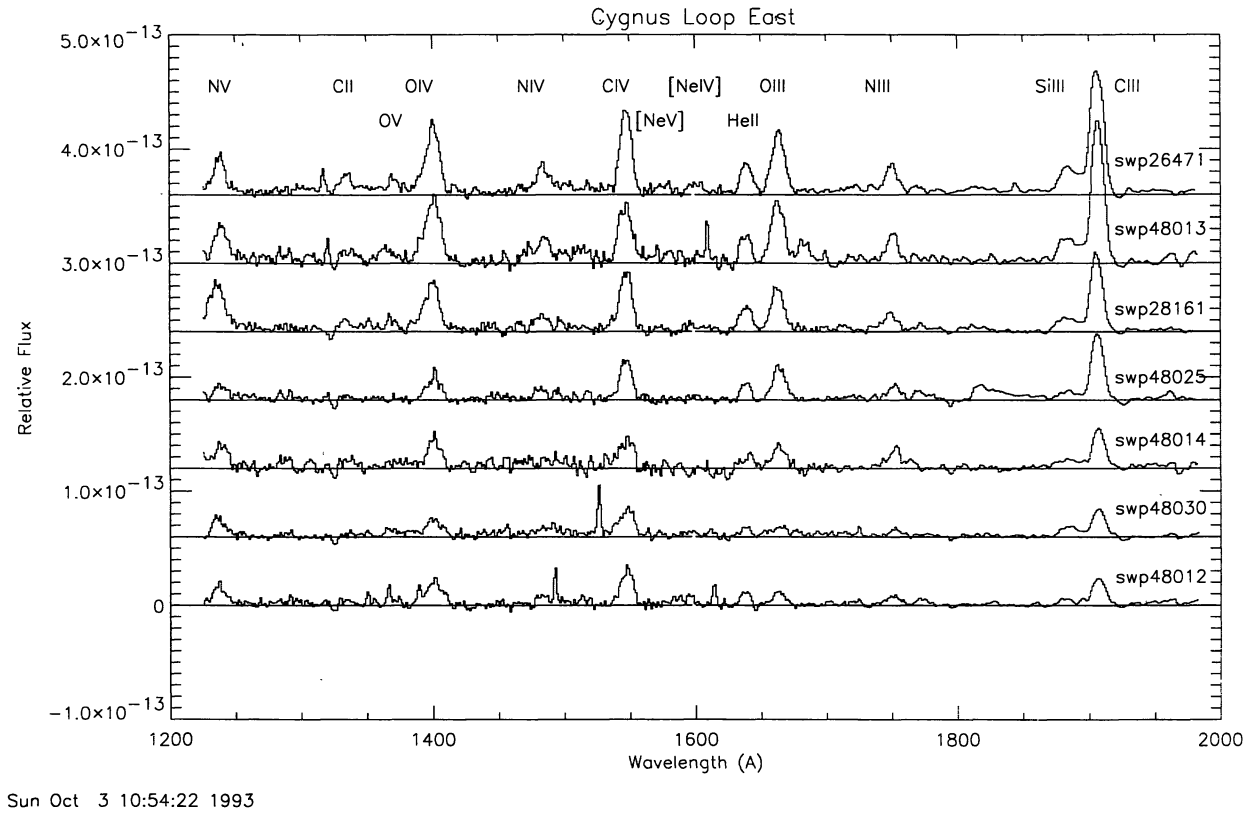

Fig. 4. UV spectra from *IUE*.

front itself or if the filaments (which are tangential to the line of sight of a somewhat rippled sheet of gas; Hester 1987) are not exactly aligned with the shock itself. Either of these might result from steep density gradients and from the large role of ram pressure as opposed to thermal pressure in driving the shock. The second problem is that the morphology does not resemble the numerical simulations of Stone & Norman (1992) or Klein, McKee, & Colella (1994) as well as might be hoped. Their models show that by the time the main blast wave has progressed 2 or 3 times the cloud diameter beyond the cloud, it will have entirely wrapped around the back of the cloud producing non-radiative shocks rather than the observed [O III] filaments. Two possible answers are that the density contrast of the XA cloud is much smaller than assumed in those simulations, or that XA is an elongated structure pointing at the center of the Cygnus Loop, perhaps the remnant of an elephant trunk structure from the H II region created by the SN precursor (Graham et al. 1995).

This work was supported by NASA Grants NAG-518 and NAG8-1074 to the Smithsonian Astrophysical Observatory.

REFERENCES

Arthur, J. A., & Henney, W. 1995, preprint
Ballet, J., Caplan, J., Rothenflug, R., Dubreuil, D., & Soutoul, A. 1989, A&A, 211, 217
Burrows, D. N., & Guo, Z. 1994, ApJ, 421, L19
Cornett, R. H. et al. 1992, ApJL, 395, L9
Cox, D. P. 1981, ApJ, 245, 534
Cox, D. P., & Smith, B. W. 1974, ApJL, 189, L105
Falle, S. A. E. G. 1995, in Shocks in Astrophysics, ed. T. J. Millar (Dordrecht: Kluwer), in press
Falle, S. A. E. G., & Garlick, A. R. 1982, MNRAS, 201, 635

Fesen, R. A., Kwitter, K. B., & Downes, R. A. 1992, AJ, 104, 719
Fesen, R. A., Blair, W. P., & Kirshner, R. P. 1982, ApJ, 262, 171
Franco, J., Tenorio-Tagle, G., Bodenheimer, P., & Różyczka, M. 1991, PASP, 103, 803
Graham, J. R., Levenson, N. A., Hester, J. J., Raymond, J. C., & Petre, R. 1995, ApJ, in press
Hester, J. J. 1987, ApJ, 314, 187
Hester, J. J., & Cox, D. P. 1986, ApJ, 300, 675
Hester, J. J., Parker, R. A. R., & Dufour, R. J. 1984, ApJ, 273, 219
Hester, J. J., Raymond, J. C., & Blair, W. P. 1994, ApJ, 420, 721
Hester, J. J., Raymond, J. C. & Danielson, G. E. 1986, ApJL, 303, L17
Jones, T. W., & Kang, H. 1993, ApJ, 402, 560
Klein, R. I., McKee, C. F., & Colella, P. 1994, ApJ, 420, 213
Levenson, N. A., Graham, J. R., Hester, J. J., & Petre, R. 1995, in preparation
Mac Low, M.-M., McKee, C. F., Klein, R. I., Stone, J. M., & Norman, M. L. 1994, ApJ, 433, 757
McKee, C. F., & Cowie, L. L. 1975, ApJ, 195, 715
McKee, C. F., & Ostriker, J. P. 1977, ApJ, 218, 148
Norman, C. A., & Ikeuchi, S. 1989, ApJ, 345, 372
Raymond, J. C., Hester, J. J., Cox, D. P., Blair, W. P., Fesen, R. A., & Gull, T. R., 1988, ApJ, 324, 869
Ryu, D., & Vishniac, E. T. 1987, ApJ, 313, 820
Shapiro, P. R., & Field, G. B. 1976, ApJ, 205, 762
Shull, P., Dyson, J. E., Kahn, F. D., & West, K. A. 1985, MNRAS, 212, 799
Slavin, J. D., Shull, J. M., & Begelman, M. C. 1993, ApJ, 407, 83
Stone, J. M., & Norman, M. L. 1992, ApJ, 390, L17
Tenorio-Tagle, G., & Różyczka, M. 1986, A&A, 155, 120
Teske, R. G., & Kirshner, R. P. 1985, ApJ, 292, 22
Vancura, O., Raymond, J. C., Dwek, E., Blair, W. P., Long, K. S., & Foster, S. 1993, ApJ, 431, 188